Journal of Materials Processing Tech. 248 (2017) 56–63

Contents lists available at ScienceDirect

Journal of Materials Processing Tech.

journal homepage: www.elsevier.com/locate/jmatprotec

The elimination of pores in laser welds of AISI 304 plate using different shielding gases

Junhao Sun[a,b], Pulin Nie[a,b], Kai Feng[a,b], Zhuguo Li[a,b,*], Baochao Guo[c], En Jiang[c]

[a] Shanghai Key Laboratory of Materials Laser Processing and Modification, School of Materials Science and Engineering, Shanghai Jiao Tong University, Shanghai 200240, China

[b] Collaborative Innovation Center for Advanced Ship and Deep-Sea Exploration, Shanghai 200240, China

[c] Shanghai No. 1 Machine Tool Works Co., Ltd, Shanghai 201308, China

ARTICLE INFO

Keywords:
Laser welding
Stainless steel
Pores
Shielding gas
Thermodynamics and kinetics models

ABSTRACT

A laser power of 10 kW was used to weld 304 stainless steel. Different shielding gases including Ar, N_2 and no gas were used. The porosity in the laser welds was examined. The metallic plume, liquid melt pool and laser keyhole were observed by a high-speed video camera. Bubbles were produced in all the laser welds. Many pores were retained in the 304L stainless steel laser welds made in Ar. Almost no pores were found in the laser welds made in N_2 or no shielding gas. The dissolution of N_2 bubbles in the liquid melt pool led to the elimination of the pores in the 304L laser welds. The retention time of liquid melt pool was 1.1 s at a laser power of 10 kW and a welding speed of 0.8 m/min. It took 30 μs to absorb all the N_2 bubbles in the liquid melt pool. The increase of the nitrogen content in weld metal was 3.4×10^{-5} wt.%.

1. Introduction

Lu et al. (2015) and Wei and Chao (2015) indicated that the formation of porosity was closely related to keyhole fluctuation. The keyhole shape and depth varied all the time and a bubble might be produced at the bottom of the liquid melt pool. If the bubble was stopped by the solidified metal when flowing up, that would result in keyhole-induced porosity.

Tsukamoto (2011) observed the keyhole variation and motion of the molten pool through high speed X-radiography, and depression at the keyhole back wall gave rise to porosity. Berger et al. (2011) performed the interaction between laser and water or ice in order to observe directly the behavior of the capillary and the flow field in the weld pool. Several different regimes of bubble generation were found and the welding velocity played an important role in the bubble formation. Zhao et al. (2011) analyzed the forces of interaction of fluid dynamics in the keyhole and molten pool using CFD software. Keyhole depth fluctuated in continuous laser welding, and the bubbles forming from keyhole collapse and shrinkage was the cause of keyhole-induced porosity.

Chang et al. (2015) established a computational fluid mechanics model for full penetration laser welding of titanium alloy. It was proposed that measures to decrease Reynolds number of the fluid flow close to the keyhole could prove effective in reducing or avoiding porosity. Matsunawa (2011) found that keyhole fluctuation in continuous wave laser welding could be suppressed by controlled pulse modulation if a suitable pulse frequency and duty cycle were selected. Matsunawa et al. (2003) showed that the porosity could be depressed in CO_2 laser welding of Al alloy using N_2 as the shielding gas because the formation of AlN in the weld metal. Kamimuki et al. (2002) indicated that side-blowing gas could compress the surface of the molten pool, making the molten pool wider and keyhole more stable, thus reducing the porosity in weld. Meng et al. (2014) observed the keyhole and molten pool dynamic behavior in laser lap welding T-joints, and porosity was suppressed by maintaining a small gap or adopting high welding speed. Zhao et al. (2014) prevented the porosity formation by oxygen addition in fiber laser and fiber laser-GMA hybrid welding. This effect was attributable to stabilization of the keyhole by oxygen.

Different shielding gases were used to eliminate the porosity in the high-power laser welds of 304 stainless steel in this study. The mechanism to reduce the porosity was revealed in detail.

2. Materials and experimental procedure

20-mm-thick type 304 austentic steel was used in the present investigation, which was provided in the form of rolled and annealed

* Corresponding author at: Shanghai Key Laboratory of Materials Laser Processing and Modification, School of Materials Science and Engineering, Shanghai Jiao Tong University, Shanghai 200240, China.
E-mail address: lizg@sjtu.edu.cn (Z. Li).

http://dx.doi.org/10.1016/j.jmatprotec.2017.05.011
Received 24 January 2017; Received in revised form 12 May 2017; Accepted 12 May 2017
Available online 13 May 2017

Table 1
Nominal chemical compositions of AISI 304.

Alloys	Elements/wt.%							
	Fe	C	Mn	Si	S	P	Cr	Ni
AISI 304L	Balance	0.027	1.6	0.36	0.002	0.01	18.5	11.6

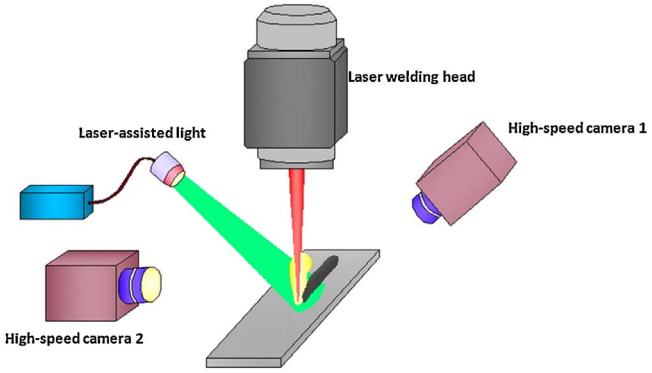

Fig. 1. Schematic diagram of the experimental set up.

state. The chemical composition of the base metal is given in Table 1.

The setup used in this experiment is shown in Fig. 1. As seen in Fig. 1, bead-on-plate weld was done on a 304L stainless steel plate with a laser keyhole welding method. A continuous wave IPG fiber laser (IPG YLS-10000) with a 10-kW maximum power and a beam parameter product of 12.5 mm mrad, was carried out to perform the laser welding, and the laser machine emitted at the near infrared spectral range (1070–1080 nm). The optical fiber laser was focused on a spot of diameter 0.72 mm through a lens of focal length 400 mm.

A standard CMOS high-speed video camera (Photron Fast cam SA4) was applied to monitor the plume and keyhole behavior. The camera was placed at different positions to observe the generation of the laser-induced plume and the formation of the keyhole. The camera 1 was directed at the process at a 90° angle between the welding direction and the camera axis, and an angle of close to 45° between laser beam and camera axis to observe the dynamic of the keyhole and the weld pool. A low power laser-assisted light (Cavilux) with a wavelength of 810 nm was used as backlight source to illuminate the welding zone to obtain clear images. An optical short-pass filter was mounted in front of the camera lens to block reflected laser light. The camera 2 was directed at the process at a 90° angle between the welding direction and the camera axis, and an angle of close to 90° between laser beam and camera axis was used to observe the dynamic of the plume. This process was carried out without filter and illumination. The welding phenomenon was recorded at a speed of 4000 frames per second.

During the laser welding experiments, the fiber laser power was set to 10 kW. The welding processes were investigated under different weld speeds and shielding gases. Shielding gases of Ar, N_2 and no gas were included. A shielding gas nozzle with an 8 mm diameter orifice was directed at the beam impingement point at a 45-deg angle and 15 L/min flow rate to protect the weld beam.

The mixed gases of Ar + N_2, which included 100% Ar, 80%Ar + 20%N_2, 60%Ar + 40%N_2, 40%Ar + 60%N_2, 20%Ar + 80%N_2 and 100% Ar were also used as the shielding gases to analyze the influence of the N_2 on the reduction of porosity formed in the high-power laser welds of 304L.

The coupons were radiographed to film to observe porosity using X-ray method. The laser welds of the cross-section and longitude-section were also cut using the wire-electrode method to observe the porosity distribution after welding. The cutting process of the longitude-section was performed by cutting the laser welds along the center line. After the cross-section and the longitude-section of the samples were produced, the porosity in the laser welds was observed by the optical microscopy.

3. Results and discussion

3.1. Porosity in laser welds

The welds were examined using X-ray method. The results are shown in Fig. 2. As seen, many line-shaped pores were formed in the center of the laser weld when using Ar. No significant porosity was found when N_2 or no shielding gas was used. The laser welds of the cross-section and longitude-section were obtained to further observe the porosity and calculate the porosity volume.

All the laser welds were carried out with a laser power of 10 kW. Different welding speeds and shielding gases were used. The obtained results are presented in Figs. 3–5. Fig. 3 shows the weld appearances, cross and longitudinal sections with no shielding gas and various welding speeds of 0.6 m/min, 1.0 m/min and 1.5 m/min. Figs. 4 and 5 show the weld appearances, cross and longitudinal sections with a welding speed of 0.8 m/min, and different shielding gases of Ar and N_2 respectively.

Fig. 3(a) displays the welding appearances with no shielding gas. As seen, all the welds' surfaces were rough and uncontinuous, which were covered with serious oxide coatings. The spreadability of the liquid melt was poor when it was seriously oxidized. The laser welds became uncontinuous with large and periodic welding scales, especially when a low welding speed of 0.8 m/min was used. Many spatters, which varied

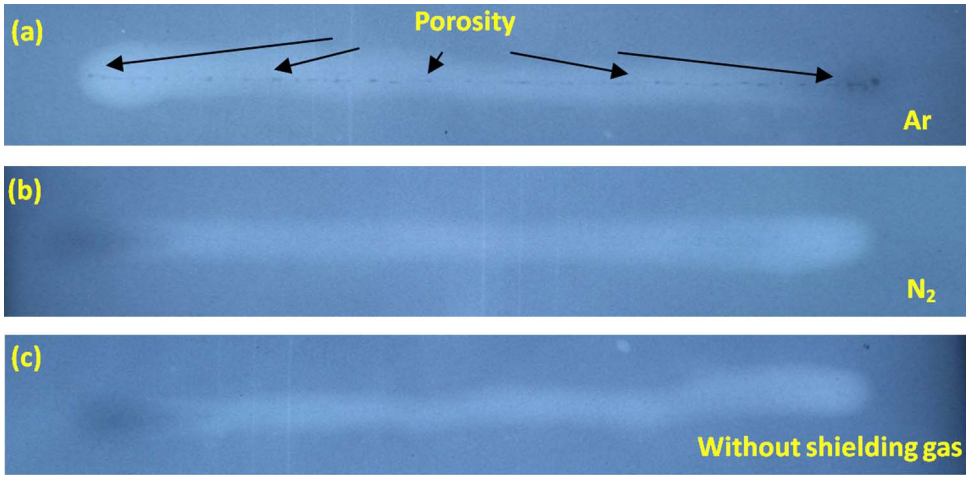

Fig. 2. Radiographs of laser weld made in 304L stainless steel with a laser power of 10 kW, a welding speed of 0.8 m/min and different shielding gases of (a) Ar, (b) N_2 and (c) no gas.